Neuron, Volume *105*

Supplemental Information

Neurons that Function within an Integrator to Promote a Persistent Behavioral State in *Drosophila*

Yonil Jung, Ann Kennedy, Hui Chiu, Farhan Mohammad, Adam Claridge-Chang, and David J. Anderson

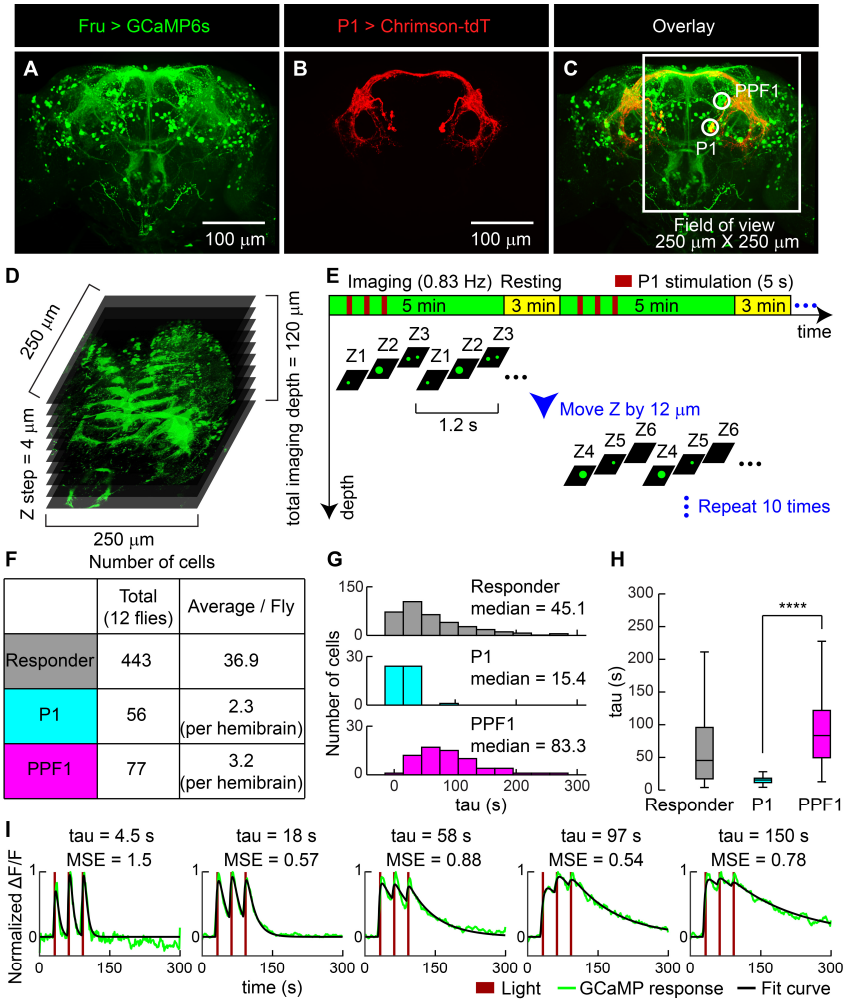

Figure S1. Volumetric functional GCaMP imaging to identify persistent P1 follower cells, related to Figure 1.

(A-C) Maximum intensity confocal stacks showing projection patterns of Fruitless (A) and P1^a (B) neurons (Hoopfer *et al.*, 2015; Anderson, 2016) expressing GCaMP6s and Chrimson-tdT, respectively; (C), overlay. (D, E) Schematics illustrating functional connectomics strategy. Responses to P1^a photostimulation (3 x 5 s pulses) from multiple Fru>GCaMP6s cells in each imaging plane (250 x 250 µm^2) were recorded during ten 5 min trials, at multiple z-depths (4 µm/z-step) covering 120 µm. (F) Number of Fruitless$^+$ cells that responded to P1^a activation. PPF1 cells were identified anatomically in high-resolution images acquired following P1 stimulation trials, using 40 mM KCl-containing saline to increase baseline GCaMP6s signals. Red channel (Chrimson-tdTomato) was used to identify P1 neurons, and cell body position and primary projection pattern were used to identify PPF1 neurons. P1 and PPF1 were visible in both hemi-brains of all specimens, but some responder cells on the lateral side appeared only in one hemi-brain (see Field of view marked in (C)). (G) Histogram of tau (decay constant of a model exponential fit to observed neural ΔF/F traces) for all responder cells (top, grey), P1 cells (middle, light blue), and PPF1 neurons (bottom, magenta). (H) Quantification and

statistical test for tau. Statistical test used was a Mann-Whitney U-test. **** $P < 0.0001$. tau from 80% of the total identified cells (MSE $\leq$2.06, 354 cells) were used for the plot (G) and quantification and statistical test (H). (I) Representative examples of GCaMP responses and tau for different responder cells. Dark red lines indicate Chrimson activation at 660 nm (3 stimulations, 5 s each, 10 Hz, 10 ms pulse-width, 25 s inter-stimulation interval).

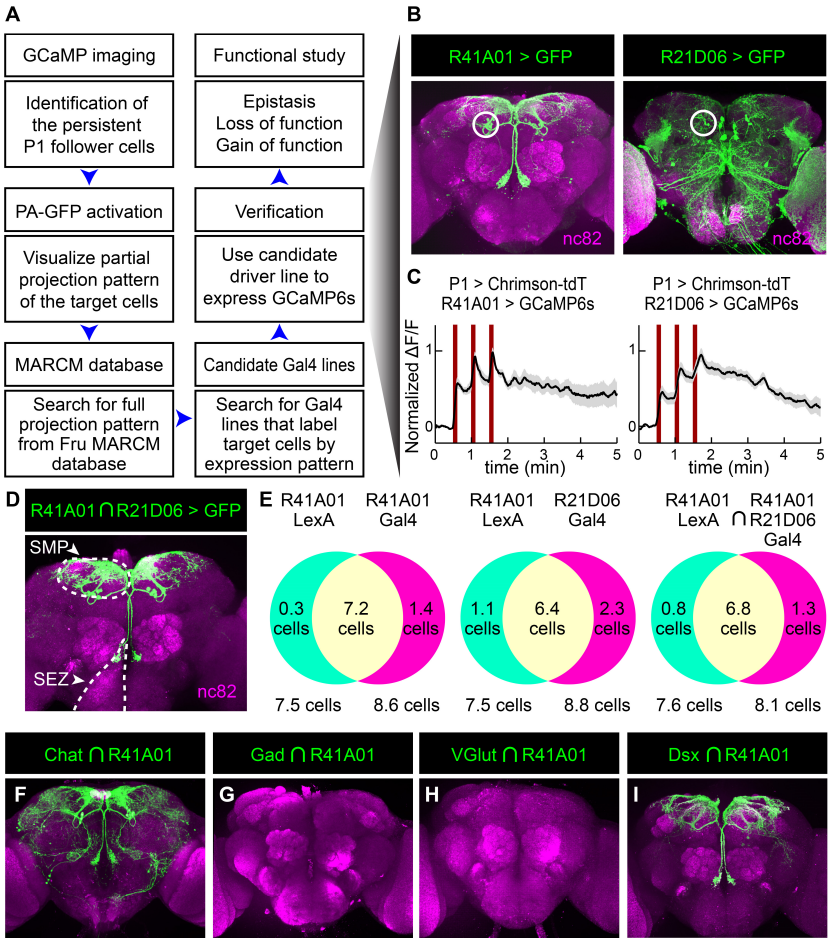

Figure S2. Gaining genetic access to PPF1 neurons and molecular phenotype of pCd neurons, related to Figure 1.

(A) Flowchart of the protocol for identifying specific Gal4 lines labeling PPF1 neurons. (B) Anatomy of two Gal4 lines, R41A01 (left) and R21D06 (right) that label PPF1 neurons. Maximum-intensity projection (z-stack) of confocal 2-μm optical sections. (C) Functional imaging of putative PPF1 neuronal cell bodies labeled by R41A01-LexA (left) and R21D06-LexA (right). Traces represent normalized ΔF/F response to P1 stimulation (dark red bars, 3 repeats of 5 s stimulation, 10 Hz, 10 ms pulse-width, 25 s inter-stimulation interval), and were obtained from cell bodies within the white circles indicated in (B). Mean±sem, n=7 (4 flies) for R41A01, and 9 (4 flies) for R21D06. (D) Anatomy of split-Gal4 intersection between R41A01-AD and R21D06-DBD in the male brain. SMP and SEZ are indicated with white dashed line. (E) Quantification of pCd cell numbers (per hemibrain) labeled by two different reporters, UAS>tdTomato and LexAop>GFP, in flies co-expressing the indicated GAL4 or LexA drivers. Green=GFP positive, Red=tdTomato positive, Yellow=double positive. Area of Venn diagram not scaled to number of cells. n=12 hemibrains per test. (F-I) Anatomy of split intersection between R41A01-AD and Chat-DBD (Diao *et al.*, 2015) (F), Gad1-AD and R41A01-DBD (G), R41A01-AD and VGlut-DBD (H), and R41A01-AD and dsx-DBD. Maximum-intensity projection of confocal 2-μm optical sections.

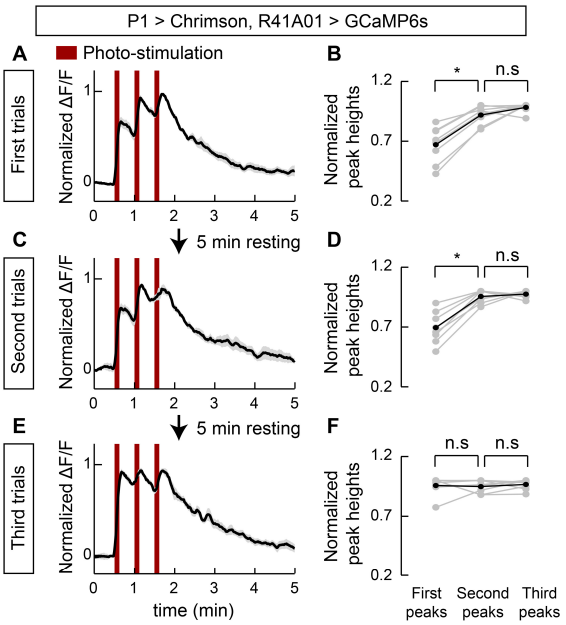

Figure S3. Integration of repeated P1 input by pCd neurons, related to Figure 1.

(A, C, E) Normalized GCaMP response of pCd neurons to optogenetic stimulation of P1 neurons. Mean±sem. n=8 cells, 6 flies. (B, D, F) Normalized peak heights during each P1 stimulation. Statistical test used was Wilcoxon signed test with correction for multiple comparisons. * $P < 0.05$

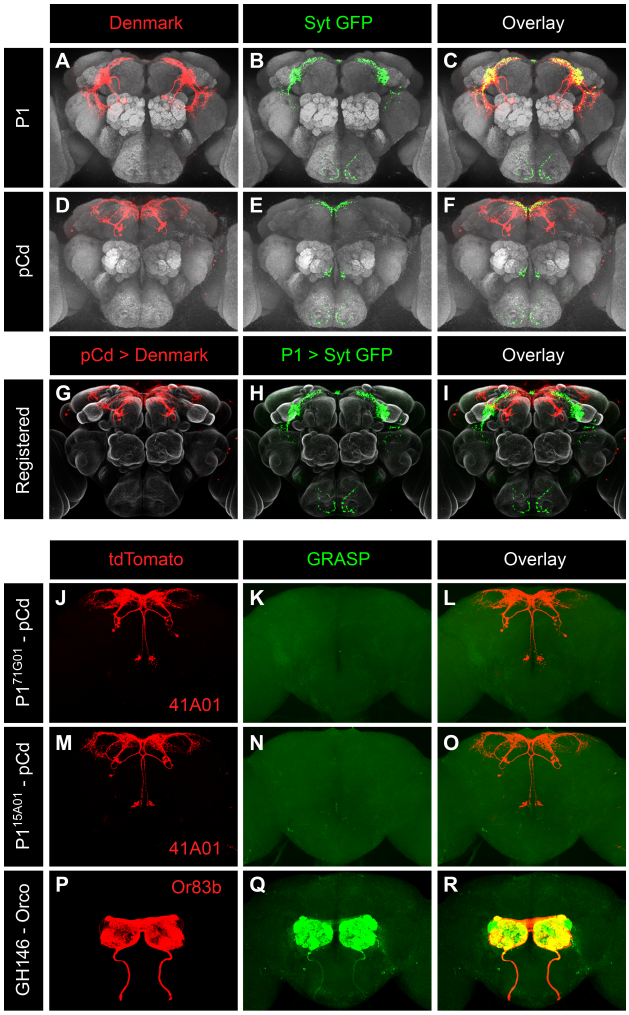

Figure S4. Anatomic relationship between P1 and pCd neurons, related to Figure 1.

(A-F) Input and output region of the P1 and pCd neurons visualized by double-labeling with somatodendritic marker (Denmark, red) and pre-synaptic marker (Syt-GFP, green). (G-I). Co-registered images showing somatodendritic region of pCd neurons and pre-synaptic region of P1 neurons. Note that yellow regions in (I, "Overlay") are not observed when the image is rotated and viewed from a different angle, indicating a lack of overlap. (J-R) GRASP (Feinberg *et al.*, 2008) experiments performed between R41A01 (pCd driver) and either of two P1 drivers, 71G01 (J-L) and 15A01 (M-O), or between GH146 and Orco as a positive control (P-R). tdTomato was expressed in one of the putative synaptic partners, R41A01 (J and M) or Orco (P), to mark fibers for detailed analysis. No positive GRASP signal is observed between pCd and either of the 2 P1 drivers (J-O).

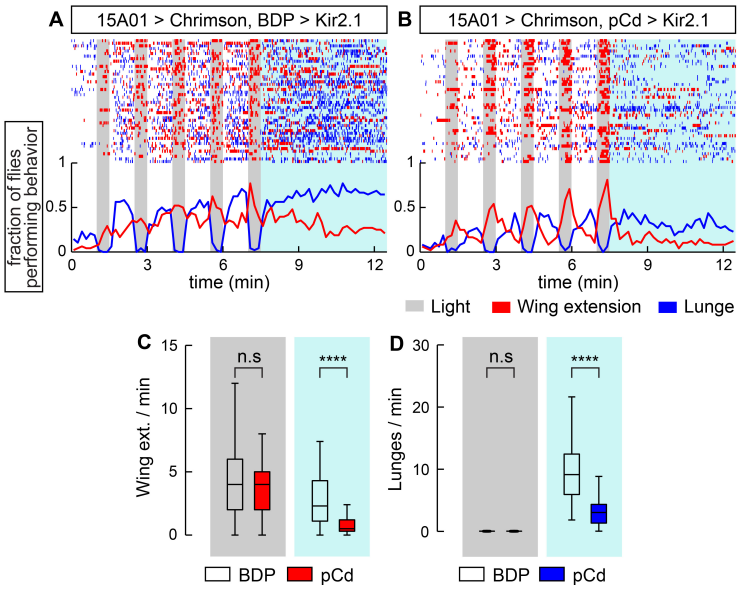

Figure S5. Inhibition of pCd neurons with R41A01∩R21D06 Split-Gal4 reduces P1-induced social behaviors, related to Figure 2.

(A, B) Top: raster plot showing wing extensions (red ticks), and lunges (blue ticks) in pair of males. In this experiment, a single driver 15A01-LexA (Hoopfer *et al.*, 2015; Watanabe *et al.*, 2017) was used to activate P1 neurons, while a split GAL4 driver (Figure S2D) was used to inhibit pCd neurons, complementing the genetic strategy used in Figure 2 in which a split-Gal4 was used to activate P1 neurons, while R41A01-LexA was used to inhibit pCd neurons (see Table 1 for genotypes). Bottom: fraction of flies performing unilateral wing extensions (red lines), and lunges (blue lines) in 10 s time bins. Gray bars indicate Chrimson activation (5 repeats of 30 s stimulation, continuous light, 60 s inter-stimulation interval). n= 48 flies per genotype. (C, D) Quantification and statistical tests for unilateral wing extensions (C) and lunges (D) during P1 stimulation (gray shading) and after photostimulation (blue shading), without (open boxes, BDP) or with (red boxes) silencing of pCd neurons using Kir2.1 . **** $P < 0.0001$ for between-genotype comparisons (Mann-Whitney U-test). Note that both wing-extensions and aggression are suppressed by pCd silencing during the post-P1 stimulation period.

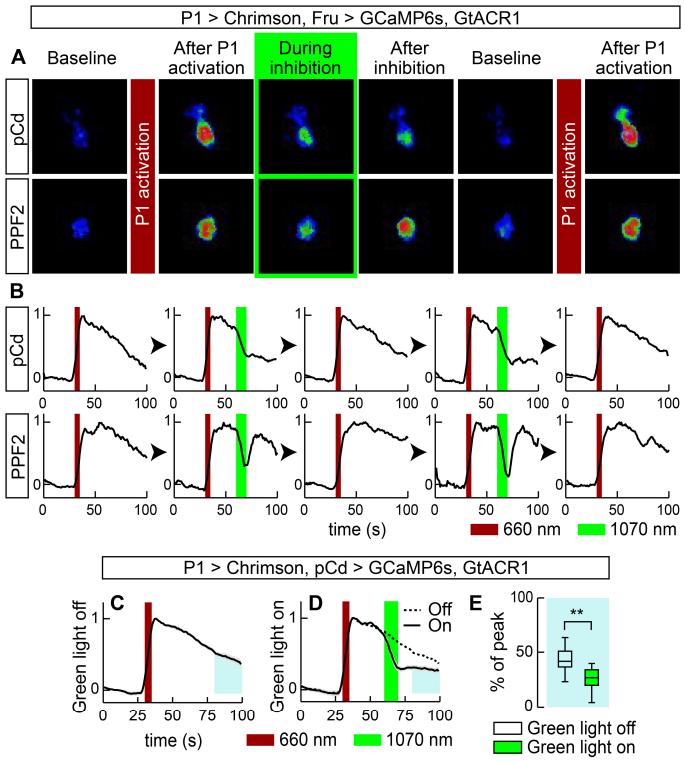

Figure S6. Multiple cycles of P1 stimulation and GtACR1 actuation, and inhibition of pCd neurons following P1 stimulation labeled by a pCd-specific driver, related to Figure 5.

(A) Representative GCaMP fluorescent images of pCd (*upper*) and PPF2 neurons (*lower*) at different time points following Chrimson-mediated P1 stimulation (wide-field LED actuation at 660 nm), and cell-restricted GtACR-mediated pCd or PPF2 inhibition (2-photon spiral scanning actuation at 1070 nm). pCd and PPF2 neurons both respond to P1 stimulation, and their response endures following offset of P1 photostimulation ("After P1 activation"). GCaMP signals in pCd neurons rapidly decrease upon photo-inhibition ("During inhibition", green outline), and do not recover 10 s following offset of GtACR actuation ("After inhibition"). In contrast, PPF2 activity recovers after photo-inhibition. pCd and PPF2 neurons were reliably reactivated by a second cycle of P1 stimulation after following GtACR-mediated inhibition. Images shown are averaged over 5 frames. (B) Representative GCaMP trace (normalized $\Delta F/F$) from individual trials. Multiple cycles of P1 stimulation with or without GtACR1 actuation did not change the initial responses of pCd and PPF2 neurons to P1 stimulation. Dark red bar indicates Chrimson activation at 660 nm (5 s, 10 Hz, 10 ms pulse-width), and green bar indicates GtACR1 actuation (~10 s, spiral scanning) 25 s after Chrimson activation. (C) GCaMP6s response of pCd neurons (normalized $\Delta F/F$) labeled with the driver R41A01-LexA (pCd^{R41A01}) to P1 stimulation (dark red bar) without GtACR1 actuation. (D) GCaMP6s response of pCd^{R41A01} to P1 stimulation with GtACR1 actuation. n=10 trials from 3 flies (C, D). Dark red bar indicates Chrimson activation at 660 nm (5 s, 10 Hz, 10 ms pulse-width), and green bar indicates GtACR1 actuation (~10 s, spiral scanning) 25 s after Chrimson activation. (E) Normalized area under the curve after photo-inhibition (blue shaded area in (C, D)).

Statistical test used was a Mann-Whitney U-test. ** $P < 0.01$. This experiment confirms the result reported in Figure 7, in which Fru-LexA was used to express GCaMP6s and pCd neurons were identified morphologically.

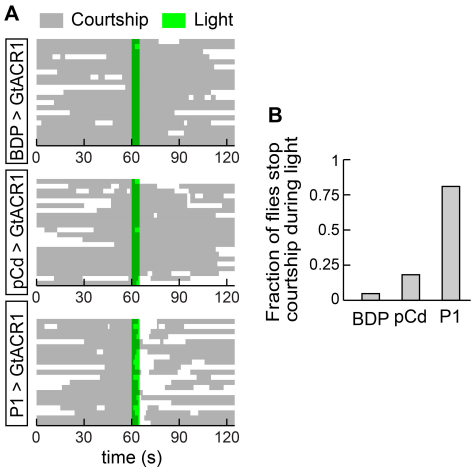

Figure S7. Transient inhibition of P1 neurons interrupt ongoing courtship behavior toward dead female, related to Figure 6.

(A) Raster plot showing courtship toward dead female (gray). Note that "courtship" metric used here incorporates multiple behavioral actions, following the definition used by Zhang et al. (Zhang *et al.*, 2018a), and thereby differs from the wing extension metric used in other figures (see Methods for details). Green line indicates GtACR1 stimulation (530 nm, 10 Hz, 10 ms pulse-width) for 10 s. n=21 for BDP and P1 > GtACR1, and 22 for pCd > GtACR1. (B) Fraction of flies stop on-going courtship behaviors during light stimulation.

Table S1. Genotypes used in this study, related to STAR Methods.

Figure	Male genotype
Figure 1A, B	w-, *10xUAS-IVS-Syn21-Chrimson::tdT3.1-SV40 (attp18)*, *13xLexAop2—Syn21-OpGCaMP6s-p10 (su(Hw)attp8)* ; *15A01-AD (attp40)*/+ ; *71G01-DBD (attp2)*/*Fru-LexA*
Figure 1C1-3	w-, *13xLexAop2-IVS-Syn21-mPA-p10 (su(Hw)attp8)* ; *15A01-AD (attp40)/13xLexAop2-IVS-Syn21-NLS-OpGCaMP6s-scalloped-NLS-p10 (su(Hw)attp5)* ; *71G01-DBD (attp2), 10xUAS-IVS-Syn21-Chrimson::tdT3.1-SV40 (su(Hw)attp1)/Fru-LexA*
Figure 1C4	w-, *13xLexAop2-IVS-Syn21-mPA-p10 (su(Hw)attp8)* ; *15A01-AD (attp40)/13xLexAop2-IVS-Syn21-NLS-OpGCaMP6s-scalloped-NLS-p10 (su(Hw)attp5)* ; *71G01-DBD (attp2), 10xUAS-IVS-Syn21-Chrimson::tdT3.1-SV40 (su(Hw)attp1)/41A01-LexA::p65 (attp2)*
Figure 1D	w- ; +/+ ; *41A01-Gal4 (attp2)/10xUAS-IVS-myr::GFP (attp2)*
Figure 1E	w-, *10xUAS-IVS-Syn21-Chrimson::tdT3.1-SV40 (attp18), 13xLexAop2—Syn21-OpGCaMP6s-p10 (su(Hw)attp8)* ; *15A01-AD (attp40)*/+ ; *71G01-DBD (attp2)/41A01-LexA::p65 (attp40, attp2, or VK00027)*
Figure 2B, F	w- ; *15A01-AD (attp40)/BDP-LexA::p65 (attp40)* ; *71G01-DBD (attp2), 10xUAS-IVS-Syn21-Chrimson::tdT3.1-SV40 (su(Hw)attp1)/13xLexAop2-IVS-Kir2.1::eGFP (VK00027)*
Figure 2C, G	w- ; *15A01-AD (attp40)/41A01-LexA::p65 (attp40)* ; *71G01-DBD (attp2), 10xUAS-IVS-Syn21-Chrimson::tdT3.1-SV40 (su(Hw)attp1)/13xLexAop2-IVS-Kir2.1::eGFP (VK00027)*
Figure 3B, E, H, K BDP>Chrimson	w- ; *BDP-AD (attp40)/20xUAS-IVS-Syn21-Chrimson::tdT3.1-SV40 (su(Hw)attp5)* ; *BDP-DBD (attp2)*/+
Figure 3B, E, H, K P1>Chrimson	w- ; *15A01-AD (attp40)/20xUAS-IVS-Syn21-Chrimson::tdT3.1-SV40 (su(Hw)attp5)* ; *15A01-DBD (attp2)*/+
Figure 3B, E, H, K pCd>Chrimson	w- ; *41A01-AD (attp40)/20xUAS-IVS-Syn21-Chrimson::tdT3.1-SV40 (su(Hw)attp5)* ; *21D06-DBD (attp2)*/+
Figure 4A-D pCd > GFP	w- ; *41A01-AD (attp4)*/+ ; *21D06-DBD (attp2)/10xUAS-IVS-syn21-GFP-p10 (attp2)*
Figure 4A-D pCd > Kir2.1	w- ; *41A01-AD (attp4)*/+ ; *21D06-DBD (attp2)/10xUAS-IVS-Kir2.1::eGFP (attp2)*
Figure 4A-D BDP > GFP	w- ; *BDP-AD (attp4)*/+ ; *BDP-DBD (attp2)/10xUAS-IVS-syn21-GFP-p10 (attp2)*
Figure 4A-D BDP > Kir2.1	w- ; *BDP-AD (attp4)*/+ ; *BDP-DBD (attp2)/10xUAS-IVS-Kir2.1::eGFP (attp2)*

Figure 5A	w- ; *20xUAS-Syn21-OpGCaMP6s-p10 (su(Hw)attp5)/41A01-AD (attp40) ; 10xUAS-IVS-Syn21-Chrimson::tdT3.1-SV40 (su(Hw)attp1)/21D06-DBD (attp2)*
Figure 5C, G1, G2, G4, G5	w-, *10xUAS-IVS-Syn21-Chrimson::tdT3.1-SV40 (attp18), 13xLexAop2—Syn21-OpGCaMP6s-p10 (su(Hw)attp8)* ; *15A01-AD (attp40)/13xLexAop2-IVS-GtACR1::eYFP-SV40 (attp40)* ; *71G01-DBD (attp2)/Fru-LexA*
Figure 5D, G3, G6	Same as Fig. 1A
Figure 6B	Canton S (+/+ ; +/+ ; +/+)
Figure 6D BDP>GtACR1	w- ; *BDP-AD (attp40)/+* ; *BDP-DBD (attp2)/ 20xUAS-IVS- GtACR1::eYFP-SV40 (attp2)*
Figure 6D pCd>GtACR1	w- ; *41A01-AD (attp40)/+* ; *21D06-DBD (attp2)/ 20xUAS-IVS- GtACR1::eYFP-SV40 (attp2)*
Figure 6D P1>GtACR1	w- ; *15A01-AD (attp40)/+* ; *71G01-DBD (attp2)/ 20xUAS-IVS- GtACR1::eYFP-SV40 (attp2)*
Figure 7C	w-, *10xUAS-IVS-Syn21-Chrimson::tdT3.1-SV40 (attp18), 13xLexAop2—Syn21-OpGCaMP6s-p10 (su(Hw)attp8)* ; *15A01-AD (attp40)/+* ; *71G01-DBD (attp2)/41A01-LexA::p65 (attp2, or VK00027)*
Figure S1	Same as Fig. 1A
Figure S2B left	Same as Fig. 1D
Figure S2B right	w- ; +/+ ; *21D06-Gal4 (attp2)/10xUAS-IVS-myr::GFP (attp2)*
Figure S2C left	Same as Fig. 1E
Figure S2C right	w-, *10xUAS-IVS-Syn21-Chrimson::tdT3.1-SV40 (attp18)*, *13xLexAop2—Syn21-OpGCaMP6s-p10 (su(Hw)attp8)* ; *15A01-AD (attp40)/+* ; *71G01-DBD (attp2)/21D06-LexA::p65 (attp2)*
Figure S2D	w- ; *41A01-AD (attp40)/+* ; *21D06-DBD (attp2)/10xUAS-IVS-myr::GFP (attp2)*
Figure S2E left	w- ; *10xUAS-IVS-NLS-tdTomato (VK00022)/+* ; *41A01-LexA::p65 (VK00027), 13xLexAop2-IVS-NLS-GFP (VK00040)/41A01-Gal4 (attp2)*
Figure S2E middle	w- ; *10xUAS-IVS-NLS-tdTomato (VK00022)/+* ; *41A01-LexA::p65 (VK00027), 13xLexAop2-IVS-NLS-GFP (VK00040)/21D06-Gal4 (attp2)*
Figure S2E right	w- ; *10xUAS-IVS-NLS-tdTomato (VK00022)/41A01-AD (attp40)* ; *41A01-LexA::p65 (VK00027), 13xLexAop2-IVS-NLS-GFP (VK00040)/21D06-DBD (attp2)*
Figure S2F	w-,*10xUAS-IVS-myr::GFP (su(Hw)attp8)* ; *41A01-AD (attp40)/+* ; *Chat-DBD/+*
Figure S2G	w-,*10xUAS-IVS-myr::GFP (su(Hw)attp8)* ; *Gad1-AD/+* ; *41A01-DBD (attp2)/+*
Figure S2H	w-,*10xUAS-IVS-myr::GFP (su(Hw)attp8)* ; *41A01-AD (attp40)/+* ; *VGlut-DBD/+*
Figure S2I	w-,*10xUAS-IVS-myr::GFP (su(Hw)attp8)* ; *41A01-AD (attp40)/+* ; *Dsx-DBD/+*
Figure S3	Same as Fig. 1E

Figure S4A-C	w- ; *15A01-AD (attp40)*/+ ; *71G01-DBD (attp2)/UAS-Denmark, UAS-Syt-eGFP*
Figure S4D-F	w- ; *41A01-AD (attp40)*/+ ; *21D06-DBD (attp2)/UAS-Denmark, UAS-Syt-eGFP*
Figure S4J-I	w-, *13xLexAop2-IVS-myr::tdTomato (attp18)* ; *41A01-LexA (attp40)/LexAop-CD4::spGFP11* ; *71G01-Gal4 (attp2)/UAS-CD4::spGFP1-10*
Figure S4M-O	w-, *13xLexAop2-IVS-myr::tdTomato (attp18)* ; *41A01-LexA (attp40)/LexAop-CD4::spGFP11* ; *15A01-Gal4 (attp2)/UAS-CD4::spGFP1-10*
Figure S4P-R	w-, *13xLexAop2-IVS-myr::tdTomato (attp18)* ; *GH146-Gal4/LexAop-CD4::spGFP11* ; *Or83b-LexA/UAS-CD4::spGFP1-10*
Figure S5A	w- ; *BDP-AD (attp40)/13xLexAop2-IVS-CsChrimson::mVenus (attp40)* ; *BDP-DBD (attp2)/15A01-LexA::p65 (attp2), UAS-Kir2.1::eGFP*
Figure S5B	w- ; *41A01-AD (attp40)/13xLexAop2-IVS-CsChrimson::mVenus (attp40)* ; *21D06-DBD (attp2)/15A01-LexA::p65 (attp2), UAS-Kir2.1::eGFP*
Figure S6A, B	Same as Fig. 5C
Figure S6C-E	w-, *10xUAS-IVS-Syn21-Chrimson::tdT3.1-SV40 (attp18), 13xLexAop2—Syn21-OpGCaMP6s-p10 (su(Hw)attp8)* ; *15A01-AD (attp40)/13xLexAop2-IVS-GtACR1::eYFP-SV40 (attp40)* ; *71G01-DBD (attp2)/41A01-LexA (attp2 or VK00027)*
Figure S7	Same as Fig. 6D

Insertion sites: attp18 (X), su(Hw)attp8 (X), su(Hw)attp5 (2R), VK00022 (2R), attp40 (2L), VK00040 (3R), VK00027 (3R), su(Hw)attp1 (3R), attp2 (3L).

Females: always wild-type Canton S (+/+ ; +/+ ; +/+)

Table S2. Statistics, related to STAR Methods.

Figure	Statistical test	Comparisons	Identifiers	p-values
Figure 1C2	Mann-Whitney U-test	NLS vs Cyto. GCaMP	n.s	0.15
Figure 2D left	Mann-Whitney U-test	BDP vs pCd	****	9.5e-13
Figure 2D right	Mann-Whitney U-test	BDP vs pCd	n.s	0.82
Figure 2H left	Mann-Whitney U-test	BDP vs pCd	****	3.6e-16
Figure 2H right	Mann-Whitney U-test	BDP vs pCd	n.s	0.11
Figure 3C during photo-stimulation	Kruskal-Wallis test	BDP vs pCd	n.a	not applicable
	Dunn's correction	BDP vs P1	****	2.5e-13
Figure 3C after photo-stimulation	Kruskal-Wallis test	BDP vs pCd	n.a	not applicable
	Dunn's correction	BDP vs P1	****	4.4e-13
Figure 3F during photo-stimulation	Kruskal-Wallis test	BDP vs pCd	****	6.6e-06
	Dunn's correction	BDP vs P1	****	1.5e-07
Figure 3F after photo-stimulation	Kruskal-Wallis test	BDP vs pCd	****	2.5e-06
	Dunn's correction	BDP vs P1	****	6.4e-09
Figure 3I after photo-stimulation	Kruskal-Wallis test	BDP vs pCd	n.s	0.58
	Dunn's correction	BDP vs P1	****	1.3e-11
Figure 3L after photo-stimulation	Kruskal-Wallis test	BDP vs pCd	****	3.0e-08
	Dunn's correction	BDP vs P1	****	7.9e-08
Figure 4B pCd	Mann-Whitney U-test	pCd>GFP vs pCd>Kir2.1	****	9.9e-07
Figure 4B BDP	Mann-Whitney U-test	BDP>GFP vs BDP>Kir2.1	n.s	0.4036
Figure 4C left total	Mann-Whitney U-test	pCd>GFP vs pCd>Kir2.1	**	0.0017
Figure 4C left first 20%	Mann-Whitney U-test	pCd>GFP vs pCd>Kir2.1	n.s	0.46
Figure 4C left last 20%	Mann-Whitney U-test	pCd>GFP vs pCd>Kir2.1	****	6.7e-06
Figure 4C right total	Mann-Whitney U-test	BDP>GFP vs BDP>Kir2.1	n.s	0.38

Figure 4C right first 20%	Mann-Whitney U-test	BDP>GFP vs BDP>Kir2.1	n.s	0.18
Figure 4C right last 20%	Mann-Whitney U-test	BDP>GFP vs BDP>Kir2.1	n.s	0.30
Figure 4D left total	Mann-Whitney U-test	pCd>GFP vs pCd>Kir2.1	****	6.4e-09
Figure 4D left first 20%	Mann-Whitney U-test	pCd>GFP vs pCd>Kir2.1	n.s	0.26
Figure 4D left last 20%	Mann-Whitney U-test	pCd>GFP vs pCd>Kir2.1	****	3.6e-07
Figure 4D right total	Mann-Whitney U-test	BDP>GFP vs BDP>Kir2.1	n.s	0.56
Figure 4D right first 20%	Mann-Whitney U-test	BDP>GFP vs BDP>Kir2.1	n.s	0.74
Figure 4D right last 20%	Mann-Whitney U-test	BDP>GFP vs BDP>Kir2.1	n.s	0.79
Figure 5H pCd	Mann-Whitney U-test	Light on vs Light off	****	6.1e-06
Figure 5H PPF2	Mann-Whitney U-test	Light on vs Light off	n.s	0.87
Figure 6D within genotype	Wilcoxon signed-rank test	BDP>GtACR1 pCd>GtACR1 P1>GtACR1	n.s **** n.s	0.80 6.79e-06 0.49
Figure 6D between genotype	Kruskal-Wallis test Dunn's correction	BDP vs pCd BDP vs P1	** n.s	0.0070 1
Figure 6D	Wilcoxon signed-rank test	cVA only vs P1+cVA	**	0.0020
Figure S1H	Mann-Whitney U-test	P1 vs PPF1	****	6.2e-18
Figure S3B	Wilcoxon signed-rank test Dunn's correction	1^{st} vs 2^{nd} 2^{nd} vs 3^{rd}	* n.s	0.011 0.15
Figure S3D	Wilcoxon signed-rank test Dunn's correction	1^{st} vs 2^{nd} 2^{nd} vs 3^{rd}	* n.s	0.011 0.65
Figure S3F	Wilcoxon signed-rank test Dunn's correction	1^{st} vs 2^{nd} 2^{nd} vs 3^{rd}	n.s n.s	1 0.65
Figure S5C during photo-stimulation	Mann-Whitney U-test	BDP vs pCd	n.s	0.56

Figure S5C after photo-stimulation	Mann-Whitney U-test	BDP vs pCd	****	2.4e-06
Figure S5D during photo-stimulation	Mann-Whitney U-test	BDP vs pCd	n.s	0.37
Figure S5D after photo-stimulation	Mann-Whitney U-test	BDP vs pCd	****	2.8e-09
Figure S8C	Mann-Whitney U-test	Light on vs Light off	**	0.0091